Elevated dissolved organic carbon biodegradability from thawing and collapsing permafrost

Benjamin W. Abbott, Julia R. Larouche, Jeremy B. Jones, William B. Bowden, Andrew W. Balser

HAL Id: hal-01118298

https://univ-rennes.hal.science/hal-01118298

Submitted on 22 Jun 2022

RESEARCH ARTICLE

Key Points:
- Dissolved organic carbon from permafrost is highly biodegradable
- Elevated biodegradability only persists during permafrost collapse
- Controls on dissolved organic carbon processing

Supporting Information:
- Readme
- Figure S1

Correspondence to:
B. W. Abbott,
bwabbott@alaska.edu

Elevated dissolved organic carbon biodegradability from thawing and collapsing permafrost

Benjamin W. Abbott[1,2], Julia R. Larouche[3], Jeremy B. Jones Jr.[1,2], William B. Bowden[3], and Andrew W. Balser[1,2]

[1]Institute of Arctic Biology, University of Alaska Fairbanks, Fairbanks, Alaska, USA, [2]Department of Biology and Wildlife, University of Alaska Fairbanks, Fairbanks, Alaska, USA, [3]The Rubenstein School of Environment and Natural Resources, University of Vermont, Burlington, Vermont, USA

Abstract As high latitudes warm, a portion of the large organic carbon pool stored in permafrost will become available for transport to aquatic ecosystems as dissolved organic carbon (DOC). If permafrost DOC is biodegradable, much will be mineralized to the atmosphere in freshwater systems before reaching the ocean, accelerating carbon transfer from permafrost to the atmosphere, whereas if recalcitrant, it will reach marine ecosystems where it may persist over long time periods. We measured biodegradable DOC (BDOC) in water flowing from collapsing permafrost (thermokarst) on the North Slope of Alaska and tested the role of DOC chemical composition and nutrient concentration in determining biodegradability. DOC from collapsing permafrost was some of the most biodegradable reported in natural systems. However, elevated BDOC only persisted during active permafrost degradation, with a return to predisturbance levels once thermokarst features stabilized. Biodegradability was correlated with background nutrient concentration, but nutrient addition did not increase overall BDOC, suggesting that chemical composition may be a more important control on DOC processing. Despite its high biodegradability, permafrost DOC showed evidence of substantial previous microbial processing, and we present four hypotheses explaining this incongruity. Because thermokarst features form preferentially on river banks and lake shores and can remain active for decades, thermokarst may be the dominant short-term mechanism delivering sediment, nutrients, and biodegradable organic matter to aquatic systems as the Arctic warms.

1. Introduction

Arctic rivers deliver between 34 and 38 Tg yr^{-1} of dissolved organic carbon (DOC) to the Arctic Ocean and surrounding basins [*Holmes et al.*, 2012]. Another 37–84 Tg yr^{-1} of DOC is delivered to inland waters but respired to the atmosphere or buried in lakes and streams before reaching the ocean [*Aufdenkampe et al.*, 2011; *McGuire et al.*, 2009]. As permafrost volume shrinks due to climate change, more of the 1670 Pg of soil organic carbon (C) contained in the permafrost region [*Tarnocai et al.*, 2009] will thaw and some portion will become available for transport to aquatic ecosystems as DOC. The quantity and quality of DOC release will depend on changes in local and regional hydrology [*Frey and McClelland*, 2009; *O'Donnell et al.*, 2012; *Tank et al.*, 2012]. The importance of this permafrost DOC to regional and global C cycles depends largely on its biodegradability—the degree to which DOC is available for uptake and mineralization by microorganisms [*McDowell et al.*, 2006]. If permafrost DOC is largely biodegradable, a larger portion will be mineralized in soil and freshwater systems before reaching the ocean, accelerating C transfer from permafrost to the atmosphere, whereas if this DOC is recalcitrant, more will reach marine ecosystems where it may persist on long time scales [*Amon and Meon*, 2004; *Bianchi*, 2011]. In Arctic and boreal systems, biodegradable DOC (BDOC) ranges from <10% in soil water from the seasonally thawed active layer to 90% for some vegetation-derived DOC [*Kalbitz et al.*, 2003; *Michaelson et al.*, 1998; *Wickland et al.*, 2007]. Riverine BDOC varies seasonally from <10 to 40% with highest biodegradability typically during snowmelt [*Holmes et al.*, 2008; *Mann et al.*, 2012; *Wickland et al.*, 2012]. However, very little is known about BDOC from thawing permafrost, with conflicting evidence showing higher and lower biodegradability compared to DOC from litter and active layer soil [*Balcarczyk et al.*, 2009; *Cory et al.*, 2013; *Vonk et al.*, 2013].

Before permafrost DOC can enter the modern C cycle, regardless of its biodegradability, it has to come into contact with surface or ground waters. Because hydraulic conductivity in Arctic mineral soil is often very low [*Frampton et al.*, 2011; *Zhang et al.*, 2000], much permafrost C may be inaccessible to hydrologic
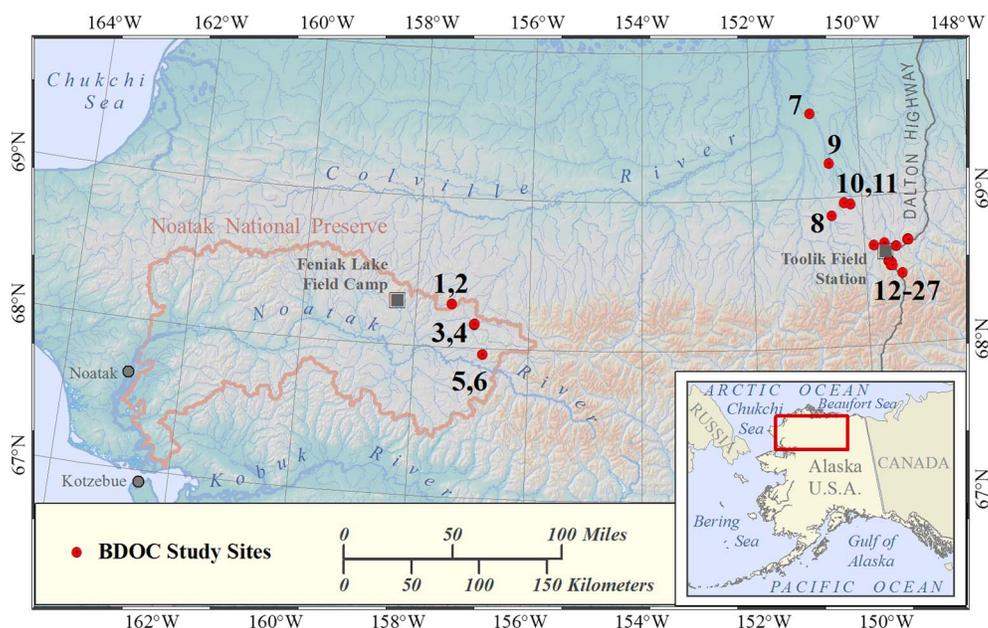
Figure 1. Map of study area.

export, even after thaw. However, in soil where ice volume exceeds pore space, permafrost thaw is accompanied by ground subsidence or thermokarst [*Jorgenson et al.*, 2008], which can rapidly mobilize sediment, nutrients, and C [*Bowden et al.*, 2008]. On hillslopes, riverbanks, and lakeshores, thermokarst can release permafrost DOC from meters below the active layer [*Vonk et al.*, 2013] and may impact watershed-level BDOC and nutrient concentrations [*Bowden et al.*, 2008; *Woods et al.*, 2011]. The term thermokarst includes a suite of thermo-erosional features with different morphologies determined primarily by ice content, substrate type, landscape position, and slope [*Osterkamp et al.*, 2009]. In upland landscapes, the three most common thermokarst morphologies are retrogressive thaw slumps, active layer detachment slides, and thermo-erosion gullies [*Jorgenson and Osterkamp*, 2005]. In addition to surface subsidence due to ground ice loss, mechanical erosion and mass wasting play a role in the formation of these features; however, we will refer to them collectively as thermokarst following literature convention [*Kokelj and Jorgenson*, 2013]. Thaw slumps have a retreating headwall and are fueled by a variety of ground ice types, active layer detachment slides form when the seasonally thawed surface layer of vegetation and soil slips downhill over an ice-rich transition zone, and thermo-erosion gullies form due to ice wedge melt, growing with a generally linear or dendritic pattern (supporting information Figure S1). These three morphologies currently impact approximately 1.5% of the landscape in the western foothills of the Brooks Range [*Krieger*, 2012] and could affect up to 30% of the North Slope of Alaska with moderate warming [*Jorgenson et al.*, 2006].

In this study we measured the biodegradability of DOC released by thermokarst across common tundra vegetation and permafrost types on the North Slope of Alaska. We hypothesized that permafrost DOC would be more biodegradable than DOC from the active layer due to two nonmutually exclusive mechanisms. First, permafrost DOC may contain more biodegradable chemical compounds due to limited prior microbial processing or differences in original vegetation sources. Second, high-nutrient concentrations in permafrost meltwater may accelerate DOC breakdown by relieving nutrient limitation of heterotrophic microorganisms. If DOC chemical composition is the main driver of biodegradability, we predicted that DOC aromaticity and the C:N ratio of dissolved organic matter (DOM) would be negatively correlated with biodegradability. If nutrient concentration is the dominant driver of DOC biodegradability, we predicted that the addition of nutrients would stimulate DOC processing, particularly at sites with low ambient nutrient concentrations. Likewise, we predicted that BDOC would differ by modern vegetation community and thermokarst type since these factors influence DOC chemical composition and nutrient concentration. We tested these hypotheses and predictions by (1) characterizing DOC composition released by thermokarst, (2) incubating DOC with

and without added nutrients, (3) comparing BDOC between feature and vegetation types, and (4) developing relationships between DOC composition, nutrient content, and BDOC.

2. Methods

2.1. Study Sites

We collected water from 19 thermokarst features and 8 reference water tracks in Arctic tundra near the Toolik Field Station and Feniak Lake (Figure 1 and Table 1). Both areas are situated in the foothills of the Brooks Range on the North Slope of Alaska. Toolik Field Station is located 254 km north of the Arctic Circle and 180 km south of the Arctic Ocean. The average annual temperature is −10°C and the average monthly temperatures range from −25°C in January to 11.5°C in July. The Toolik area receives 320 mm of precipitation annually with 200 mm falling between June and August [*Toolik Environmental Data Center Team*, 2011]. Feniak Lake is located 360 km west of Toolik in the central Brooks Range at the northeast boarder of the Noatak National Preserve. The Feniak Lake region receives more precipitation than the Toolik area with annual average precipitation at 450 mm [*Western Regional Climate Center*, 2011]. Both Toolik and Feniak Lake are underlain by continuous permafrost with glacial till, bedrock, and loess parent materials ranging in age from 10 to 400 ka [*Hamilton*, 2003].

2.2. Sample Collection and Analysis

We collected water from thermokarst feature outflows and reference water tracks near the Toolik Field Station (June to August in 2011 and August 2012) and near Feniak Lake (July 2011). In the Toolik area we sampled eight retrogressive thaw slumps (hereafter thaw slump), one active layer detachment slide, six thermo-erosion gullies (hereafter gully), and six reference water tracks. In the Feniak area we sampled two thaw slumps, one active layer detachment slide, one gully, and two reference water tracks. At each site, we collected four replicate samples from the main channel, which we filtered (0.7 μm effective pore size, Advanctec GF-75) into 250 mL amber low-density polyethylene (LDPE) bottles for transport to the lab where we performed photometric analysis and set up incubations within 24 h of collection. For most sites a 60 mL high-density polyethylene (HDPE) bottle for background nutrient concentrations was also filtered (0.7 μm) in the field and frozen upon return to the lab until analysis, typically within 3 months.

We measured DOC with a Shimadzu TOC-5000 connected to an Antek 7050 chemiluminescent detector to quantify total dissolved nitrogen (N) after combustion to NO_x. We characterized DOC composition by UV absorbance at 254 nm ($SUVA_{254}$), a photometric measure of DOC aromaticity [*Weishaar et al.*, 2003], and the C:N of DOM, an indicator of DOM source and degree of prior processing [*Amon et al.*, 2012]. UV absorbance was measured on a Shimadzu UV-1601 using a 1.0 cm quartz cell, and $SUVA_{254}$ was calculated by dividing UV absorbance by DOC concentration. NO_3^-, NH_4^+, PO_4^{3-}, and K were analyzed on a Dionex DX-320 ion chromatograph. Dissolved organic N (DON) was calculated by subtracting inorganic N (NO_3^-, NH_4^+, and NO_2^-) from total dissolved N. To distinguish rain from snowmelt and permafrost meltwater, δD and $\delta^{18}O$ were analyzed on a Picarro L1102-i via cavity ring-down spectroscopy.

2.3. BDOC Assays

DOC biodegradability is the degree to which DOC is available for uptake and mineralization by microorganisms. Operationally, biodegradable DOC (BDOC) is often defined as the percent DOC mineralized or taken up over a certain time period, usually 7–40 days [*McDowell et al.*, 2006], though DOC breakdown can also be characterized by single or multiple exponential models [*Wickland et al.*, 2007]. We assessed DOC biodegradability by DOC drawdown after 10 and 40 days. After initial collection and filtration in the field, 31 mL aliquots from each field bottle were filtered through 0.22 μm polyethersulfone membrane filters (Sterivex GP 0.22, Millipore) to remove bacteria and were placed in 70 mL glass incubation vials. To control for variability in microbial community among sites, we made a common inoculum by shaking the 0.22 μm filters from all sites with 100 mL of deionized water and allowing them to soak for 30 min. Prior to initial sampling, 1 mL of this bacterial inoculum was added to each incubation vial. In 2011, all vials received a nutrient amendment, increasing ambient concentrations by 80 μM NH_4^+/NO_3^- and 10 μM PO_4^{3-} [*Holmes et al.*, 2008], to relieve potential nutrient limitation of DOC processing and facilitate comparison with other studies [*McDowell et al.*, 2006]. In 2012, we compared DOC drawdown between amended and ambient nutrient incubations performed in tandem to test the effect of added nutrients on DOC processing. Samples were stored in the dark at room temperature for the

Table 1. Summary of Site Characteristics Including DOC Concentration and Biodegradability, Feature Type, Vegetation, and Ecotype[a]

Site ID	Average BDOC (%)	Average DOC (μM)	SUVA$_{254}$	Activity Index[b]	No. Times Sampled	Primary Ground Ice Type	Tundra Vegetation[c]	Ecotype[d]	Map ID	Coordinates (UTM)
ALD 1	21.1	219	1.38	2	1	Transition/Glacial	Low to tall shrublands[e]	4	24	68.4704–149.3435
ALD 2	38.5	344	2.40	3	1	Transition	Moist nonacidic tundra[e]	1	1	68.2866–157.3640
GLY 1	14.8	1159	8.42	3	4	Ice wedge	Moist acidic tundra	3	19	68.5435–149.5225
GLY 2	21.4	1180	3.71	3	4	Ice wedge(Pleistocene)	Moist acidic tundra	3	26	68.6923–149.2067
GLY 3	12.0	1946	ND	1	1	Ice wedge	Moist acidic tundra[e]	3	9	69.2278–150.5534
GLY 4	21.5	608	4.11	3	1	Ice wedge (Pleistocene)	Dwarf to low shrublands[e]	3	3	68.1589–156.9533
GLY 5	28.1	1498	3.90	1	3	Ice wedge (Pleistocene)	Moist acidic tundra	2	15	68.5524–149.5652
GLY 6	29.7	1075	3.33	2	3	Ice wedge	Moist acidic tundra	2	17	68.5541–149.5577
GLY 7	34.6	469	3.70	2	1	Ice wedge	Dwarf to low shrublands	2	23	68.6523–149.4202
TS 1	10.6	4036	2.41	3	1	Glacial/Lacustrine	Moist acidic tundra[e]	3	11	68.9514–150.1943
TS 2	56.3	1707	0.97	1	1	Glacial	Moist nonacidic tundra	4	8	68.8793–150.5563
TS 3	39.1	7943	0.77	2	2	Glacial/Lacustrine	Moist acidic tundra[e]	3	10	68.9614–150.3154
TS 4	50.0	667	2.12	1	2	Glacial	Dwarf to low shrublands	3	14	68.5554–149.5747
TS 5	36.1	612	1.96	3	1	Pore ice	Moist nonacidic tundra[e]	3	12	68.6666–149.8188
TS 6	24.2	434	1.75	3	2	Glacial	Low to tall shrublands	4	13	68.6784–149.6242
TS 7	59.2	5750	0.95	1	3	Ice wedge (Yedoma)	Moist nonacidic[e]	2	7	69.5683–150.8701
TS 8	26.3	359	1.22	1	1	Glacial	Dwarf to low shrublands[e]	3	18	68.5254–149.5438
TS 9	34.8	983	1.28	1	1	Glacial/Lacustrine	Moist nonacidic tundra[e]	3	6	67.9620–156.7889
TS 10	39.6	1225	0.97	1	1	Glacial/Lacustrine	Moist nonacidic tundra[e]	4	5	67.9619–156.7920
WT 1	9.5	740	4.40	0	4	na	Sedge, moss tundra (fen)	1	20	68.5442–149.5214
WT 2	13.2	1043	7.27	3	4	na	Sedge, moss tundra (poor fen)	3	25	68.6911–149.2084
WT 3	38.6	356	2.39	3	1	na	Moist nonacidic tundra[e]	1	2	68.2867–157.3627
WT 4	21.7	509	3.75	0	1	na	Low to tall shrublands[e]	1	4	68.1594–156.9451
WT 5	11.4	892	4.48	0	2	na	Moist nonacidic tundra	2	16	68.5537–149.5588
WT 6	8.9	439	2.62	0	1	na	Low to tall shrublands	2	22	68.6515–149.4223
WT 7	10.9	907	2.89	0	1	na	Moist acidic tundra	1	21	68.5270–149.5110
WT 8	19.2	701	4.81	0	2	na	Low to tall shrublands	3	27	68.6906–149.1922

[a]BDOC (%) determined by DOC loss during a 40 day lab incubation in the dark at 20°C with added nutrients; SUVA$_{254}$ = specific UV absorbance at 254 nm (L mg C^{-1} m^{-1}); ND = no data.
[b]Activity index is defined as 0, no apparent present or past thermo-degradation; 1, active thermo-degradation (>25% of headwall is actively expanding) with completely turbid outflow; 2, moderate thermo-degradation (<25% of headwall is expanding) with somewhat turbid outflow; and 3, stabilized or limited thermo-degradation with complete or partial revegetation and clear outflow.
[c]*Walker et al.* [2005] unless otherwise noted.
[d]Ecotype definitions follow [*Jorgenson et al.*, 2009] and coded as 1, Alpine Wet Sedge Meadow; 2, upland Birch-Willow Low Shrub; 3, upland Dwarf Birch-Tussock Shrub; and 4, upland Sedge-Dryas Meadow.
[e]This study.

duration of the incubation. Incubation vials were tightly capped to limit evaporation but were opened and wafted weekly to ensure adequate oxygen supply.

To quantify DOC loss, we sampled each vial 3 times during the incubation, at day 0, day 10, and day 40 (t_0, t_{10}, and t_{40}, respectively). At samplings, 5 mL was drawn from each vial, filtered (0.22 μm) into acid-washed, glass scintillation vials, and acidified with 100 μL of 2 N HCl to remove inorganic C and kill any residual bacteria not removed during filtration. Because this method removes microbial biomass before measuring DOC, the change in DOC concentration represents DOC loss due to both mineralization and microbial uptake. Acidified samples were stored tightly capped in the dark at room temperature until analysis within 3 months. Average DOC concentration of the four analytical replicates for each site and sampling time step was used to calculate loss. Analytical replicates with evidence of contamination or analytical error were excluded from the means, though this occurred less than 5% of the time and never resulted in dropping a site or sampling time step.

Because no single metric of DOC biodegradability is agreed upon as the most ecologically relevant, we characterized DOC biodegradability in several ways. We hereafter refer to the DOC loss by t_{40} as biodegradable DOC (BDOC), and further separate fast BDOC as loss from $t_0 - t_{10}$ and slow BDOC as loss from $t_{10} - t_{40}$. We refer to DOC remaining at t_{40} as recalcitrant. To compare fast and slow BDOC in a single metric we calculated the proportion of fast BDOC (fast BDOC μM/total BDOC μM). The 10 day increment for fast BDOC corresponds to the average stream transport time of 10.9 days (range of 3-20 days) for rivers in the study area based on average stream velocity and channel length [*Dery et al.*, 2005; *McNamara et al.*, 1998]. Because this simplified estimate of residence time does not include transient storage within the channel or layovers in lakes and estuaries, the 40 day increment may better represent typical transit time from headwater to sea.

2.4. Nutrients and DOC Chemical Composition

We used Pearson product-moment correlation and multiple linear regression to compare the relative importance of nutrients and DOC composition to BDOC. All regression and correlation analyses were based on BDOC data from nutrient amended incubations and therefore test indirect correlations between nutrients and other factors such as vegetation type, flow path, DOM source, or micronutrients rather than direct effects of N or phosphorus (P) on BDOC. We compared the explanatory power of NH_4^+, NO_3^-, PO_4^{3-}, K, $\delta^{18}O$, $SUVA_{254}$, DOC: DON, DOC:DIN, and thermokarst activity level (defined below) in predicting fast, slow, and total BDOC. Activity was recoded low to high and treated as a continuous variable for correlations but was excluded from other analyses since it is nonparametric and was highly correlated with both potassium (K) and ammonium (NH_4^+). Akaike information criterion (AIC) was used to identify the most parsimonious models and rank predictors within each model. To determine differences between amended and ambient nutrient treatments for fast, slow, and total BDOC, we applied a single population two-way t test.

2.5. Thermokarst Activity, Type, and Vegetation

To understand the release of BDOC as thermokarst features develop through time, we classified features on a 0–3 activity index based on turbidity of outflow, rate of thermo-degradation, and state of revegetation. This qualitative index uses space for time substitution to follow the development of a hypothetical feature from before initiation (0) to after stabilization (3). Activity levels are defined as follows: 0, no apparent present or past thermo-degradation; 1, active thermo-degradation (>25% of headwall is actively expanding) with completely turbid outflow; 2, moderate thermo-degradation (<25% of headwall is expanding) with somewhat turbid outflow; 3, stabilized or limited thermo-degradation with complete or partial revegetation and clear outflow. We performed a one-way analysis of variance (ANOVA), testing for differences in BDOC between thermokarst activity levels, and applied Tukey's honest significant difference to determine significant differences.

Because vegetation community influences both active layer and permafrost DOC composition and nutrient concentration, we grouped sites into three broad vegetation classes (Table 1): moist acidic tundra, moist nonacidic tundra, and shrub tundra. We tested for differences in total BDOC, $SUVA_{254}$, C:N, and nutrient concentration between the three vegetation types. Because feature activity varied between classes, we tested for differences between vegetation classes with an analysis of covariance (ANCOVA) that compared adjusted means after controlling for activity. To test how ground ice type and thermokarst morphology influence BDOC, we performed an ANCOVA comparing BDOC from gullies and thaw slumps independent of
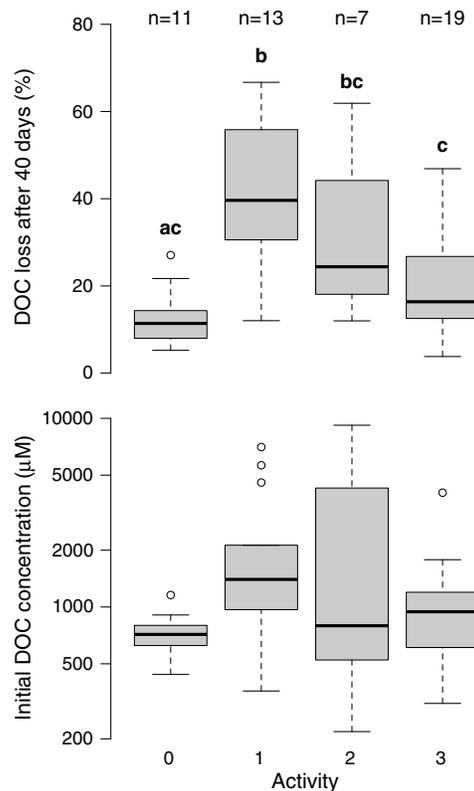
Figure 2. DOC loss in water from collapsing permafrost and reference water tracks after 40 days of lab incubation at room temperature with added nutrients and initial DOC concentration. See Table 1 or text for complete definition of activity index but 0 = reference, 1 = most active, and 3 = stabilized. Box plots represent median, quartiles, minimum and maximum within 1.5 times the interquartile range, and outliers beyond 1.5 interquartile range. Different letters represent significant differences in BDOC between activity levels, $\alpha = 0.05$. Note the log scale for DOC concentration.

activity. Comparisons with active layer detachment slides or more involved vegetation classifications such as ecotype [*Jorgenson et al.*, 2009] were not possible due to limited sample size.

2.6. Seasonal Changes in BDOC

To quantify seasonal variability of BDOC, repeat measurements were taken at the four most accessible sites (two gullies and adjacent water tracks) 4 times from 15 June to 18 August 2011, and repeat measurements were taken opportunistically at seven other sites. A two-way *t* test for unequal variance was performed on the range (maximum–minimum) of BDOC to compare variability at impacted and reference sites through the 2011 season.

2.7. Additional Statistics

Repeat measurements from four features (two gullies, one thaw slump, and one water track) were included in the regression analysis as independent samples because of substantial variability in BDOC and chemistry between sample dates, which were more than 2 months apart in every case. Repeat measurements from 12 sites (four gullies, four thaw slumps, and four water tracks) were also included as independent samples in ANOVAs and ANCOVAs for the same reasons and to capture seasonal variability in biodegradability and water chemistry.

For all analyses, we evaluated normality with normal probability plots and equal variance by plotting observed values against residuals. For multiple linear regression models, highly correlated predictors were removed prior to running the full model or applying AIC, and in addition to visual assessment, variance inflation factor, RESET, Breusch-Pagan, and Durbin-Watson tests were used to check colinearity, linearity, equal variance, and autocorrelation, respectively. Variables were natural log transformed, raised to the 0.25 exponent, and/or were centered on zero by subtracting the mean when necessary to meet these assumptions. For ANCOVA analysis, homogeneity of regression slopes was checked with interaction plots between site activity and the variable of interest. A polynomial term for $\delta^{18}O$ was included to capture the nonlinear relationship with BDOC due to depleted $\delta^{18}O$ both in snowmelt early in the season and ground ice in the middle to late season. All statistical tests were evaluated with $\alpha = 0.05$, and analysis was performed in *R* (version 3.0.2). See acknowledgments for access to the complete data set.

3. Results

3.1. Site Activity

Sites occurred on a variety of tundra vegetation and permafrost types and exhibited a range of activity levels (Table 1). Thermokarst increased BDOC relative to reference waters, with greatest impact at the most active features with concentrations approaching reference in the more stable features (Figure 2 and Table 2). DOC loss exceeded 50% after 10 days at several sites and reached 67% loss after 40 days at thaw slump 7 located in Pleistocene-aged yedoma. Total BDOC varied significantly by activity ($F(3,46) = 9.09$, $p < 0.001$) with means of 12.8, 40.9, 31.8, and 20.6% for activity levels 0–3, respectively (Figure 2 and Table 2). BDOC of the two highest

Table 2. Carbon, Nitrogen, and Water Chemistry Parameters by Thermokarst Activity Level[a]

	0			1			2			3		
Activity Level	Median	Mean	SE	Median	Mean	SE	Median	Mean	SE	Median	Mean	SE
Parameter												
DOC	716	727	59	1400	2254	588	796	2828	1363	943	1071	189
BDOC (%)	11.4	12.8	2.0	39.6	40.9	4.7	24.4	31.8	7.3	16.4	20.6	2.8
Proportion fast	0.67	0.66	0.09	0.52	0.48	0.06	0.55	0.57	0.09	0.59	0.61	0.05
DON	17.0	16.6	2.21	71.8	109.5	36.2	22.9	145.0	124.9	22.3	26.3	5.64
DOC:DON	40.4	41.2	3.55	20.7	21.7	1.51	20.5	23.7	5.10	32.0	35.4	3.68
NO_3^-	0.10	2.32	2.19	2.73	3.61	0.81	2.74	4.87	3.48	0.21	4.87	3.48
NH_4^+	1.64	1.63	0.26	35.3	64.5	18.7	33.5	25.1	11.9	2.05	4.35	2.00
PO_4^{3-}	0.009	0.015	0.008	0.156	0.242	0.082	0.054	0.144	0.094	0.036	0.063	0.020
$SUVA_{254}$	4.26	4.13	0.29	1.25	1.94	0.38	3.09	2.64	0.52	4.52	4.97	0.70
$\delta^{18}O$	−20.495	−20.932	1.04	−1.569	−22.927	1.304	−22.880	−22.804	0.614	−19.550	−19.227	0.626

[a]For activity levels 0–3, $n = 11$, 13, 7, and 19, respectively. BDOC (%) determined by DOC loss during a 40 day laboratory incubation in the dark at 20°C with added nutrients (80 μM NH_4^+/NO_3^- and 10 μM PO_4^{3-}). Proportion fast is the proportion of total BDOC loss that occurred during the first 10 days of the incubation. All concentrations are in μM. $SUVA_{254}$ = specific UV absorbance at 254 nm (L mg C^{-1} m^{-1}). See Table 1 for definition of activity levels.

activity levels differed significantly from reference water tracks ($p < 0.001$ and $p = 0.02$), but there was no significant difference in BDOC between stabilized sites and reference water tracks (levels 3 and 0; $p = 0.31$).

DOC concentrations from active thermokarst features (levels 1 and 2) were highly variable with average concentration over 3 times higher than in reference water tracks (Table 2). Differences in DON were even more pronounced with concentrations in active features nearly 8 times higher than reference concentrations. Consequently, C:N of DOM for active features was half that of reference sites. Similarly, $SUVA_{254}$ values at impacted sites were half as high as in reference waters, indicating less aromatic DOC compounds in thermokarst outflow. Nutrient concentrations were generally much higher in thermokarst water (70, 39, and 15 times higher for K, NH_4^+, and PO_4^{3-}, respectively), though NO_3^- concentration in the most active features was only 1.3 times higher than reference waters. Rainwater was enriched in $\delta^{18}O$ (−16.56‰, SD = 3.46) relative to ground ice from feature headwalls (−24.11‰, SD = 3.98) and snow meltwater (−27.58‰, SD = 3.15).

Table 3. Correlations Between Water Chemistry Parameters, Site Activity, and DOC Biodegradability[a]

	Activity	Fast BDOC (ln %)	Slow BDOC (%)	Total BDOC (%)	Total BDOC (ln μM)
	Metrics of DOC Biodegradability				
Fast BDOC (ln %)	0.33 *				
Slow BDOC (%)	0.72 ***	0.27			
Total BDOC (%)	0.62 ***	0.82 ***	0.68 ***		
Total BDOC (ln μM)	0.59 **	0.58 ***	0.68 ***	0.81 ***	
	Predictor Variables				
Initial DOC (ln μM)	0.35 *	0.17	0.41 **	0.41 **	0.84 ***
$SUVA_{254}$ (ln (L mg C^{-1} m^{-1}))	−0.56 ***	−0.54 ***	−0.45 **	−0.62 ***	−0.52 ***
DOC:DON	−0.73 ***	−0.51 **	−0.66 ***	−0.62 ***	−0.68 ***
NH_4^+ (ln μM)	0.82 ***	0.37 *	0.68 ***	0.66 ***	0.66 ***
NO_3^- (μM)$^{0.25}$	0.55 **	0.28	0.2	0.28	-0.03
DIN (μM)	0.60 ***	0.47 ***	0.48 **	0.64 ***	0.64 ***
PO_4^{3-} (μM)$^{0.25}$	0.60 ***	0.64 ***	0.67 ***	0.78 ***	0.68 ***
K (ln μM)	0.85 ***	0.50 **	0.64 ***	0.64 ***	0.59 ***
^{18}O (ln (δ^2))	0.05	0.39 *	0.02	0.31	0.29
^{18}O (δ)	−0.31	−0.23	−0.11	−0.3	−0.36 *
DOC:DIN (ln)	−0.49 **	−0.31	−0.08	−0.27	0.00

[a]Relationships were visually inspected and transformed when necessary to meet the assumption of linearity (transformation used noted for each unit in the left column). Strength of relationship was determined by Pearson product-moment correlation.
*$p < 0.05$.
**$p < 0.01$.
***$p < 0.001$.

Table 4. Multiple Linear Regression Models for Four Metrics of DOC Biodegradability[a]

Variable	Equation	R^2	F
Fast BDOC (ln %)	$-0.36 \ln(\text{SUVA} + 0.25) + -0.021\ (\text{DOC:DON}) + 0.20 \ln((\delta^{18}O + 21.2)^2) - 0.60 \ln[\text{DOC}] + 2.52\ [\text{PO}_4]^{0.25} + 6.1$	0.67	12.4
Slow BDOC (%)	$9.48\ [\text{PO}_4]^{0.25} - 2.57 \ln(\text{SUVA} + 0.25) + 4.87 \ln[\text{DOC}] + 3.30 \ln[\text{NH}_4] + 1.50\ (\delta^{18}O + 21.2) - 22.8$	0.70	13.9
Total BDOC (%)	$28.2\ [\text{PO}_4]^{0.25} + 3.46 \ln((\delta^{18}O + 21.2)^2) - 8.84 \ln(\text{SUVA} + 0.25) + 0.616\ (\delta^{18}O + 21.2) + 6.35 \ln[\text{NH}_4] + 4.57$	0.79	21.5
Total BDOC (ln μM)	$0.054\ (\delta^{18}O + 21.2) - 0.023\ (\text{DOC:DON}) + 0.188 \ln((\delta^{18}O + 21.2)^2) + 0.385 \ln[\text{NH}_4] + 2.51\ [\text{PO}_4]^{0.25} + 3.56$	0.83	27.8

[a]Multiple linear regression models were selected for fast, slow, and total BDOC (%) from full models with the following predictors: initial DOC, SUVA_{254}, DOC:DON, NH_4^+, PO_4^{3-}, and $\delta^{18}O$. For total BDOC concentration, initial DOC was excluded as a predictor since it is a part of the response variable. Stepwise AIC was used to compare full models against models with subsets of predictors with lowest AIC score determining final models. Predictors are ordered within each model from lowest to highest individual AIC ranking. $\delta^{18}O$ was centered on zero before analysis by subtracting the mean (-21.1993), and a polynomial term was included to reflect the dual sources of depleted oxygen (snow and permafrost meltwater). Models including the following terms were < 2 AIC units different than the final model (suggesting equal power and parsimony): fast BDOC (%) including NH_4^+, slow BDOC (%) including DOC:DON, total BDOC (%) including initial DOC, and total BDOC (ln uM) excluding polynomial $\delta^{18}O$ term. For all regressions $n = 29$ and $p < 0.0$.

The proportion fast BDOC (fast BDOC/total BDOC) did not vary significantly with thermokarst activity ($p = 0.24$, $n = 50$, SE $= 0.34$), with an overall average of 0.58 of the total DOC loss occurring by t_{10} (Figure 1). However, the proportion fast BDOC varied widely among individual sites, from less than 0.01 to 1.0.

3.2. Nutrients and DOC Chemical Composition

We used correlation and multiple linear regression to assess the strength of associations between nutrients and DOC composition with DOC biodegradability. Pearson product-moment correlations revealed moderate to strong relationships between the four metrics of BDOC and both DOC chemical composition and nutrient concentration (Table 3). Individual parameters were correlated with fast, slow, and total BDOC (%) as well as total BDOC concentration (μM). PO_4^{3-} had the strongest positive correlation with both fast and total BDOC, and PO_4^{3-} and C:N were equally correlated with total BDOC concentration. Thermokarst activity had the strongest relationship with slow BDOC. Fast BDOC was not significantly correlated with slow BDOC (Pearson's $r = 0.27$, $n = 50$, $p = 0.054$). All parameters, except the $\delta^{18}O$ terms, were correlated with thermokarst activity, with K and NH_4^+ expressing the strongest relationships (Pearson's $r = 0.85$ and 0.82, respectively, $n = 27$, $p < 0.001$; Table 3).

Multiple linear regression models accounted for 67–83% of the variation in the four metrics of BDOC, with chemical composition, nutrient content, and water isotopes all included as significant predictors in the various models (Table 4). PO_4^{3-} and NH_4^+ were retained after stepwise AIC for all four of the BDOC metrics, with SUVA_{254} and $\delta^{18}O$ making three of the four final models (Table 4). Most predictors were individually significant ($\alpha < 0.05$) in their specific model with the exception of SUVA_{254} and C:N in the fast BDOC model; DOC, PO_4^{3-}, and SUVA_{254} in the slow BDOC model; and C:N and $\delta^{18}O$ in the BDOC concentration model ($p = 0.07$, 0.06, 0.07, 0.16, 0.13, 0.06, and 0.25, respectively). However, these terms were retained in the final models since they improved the AIC score and were not overly correlated with other predictors in their models. The model estimating fast BDOC had the weakest relationship with measured BDOC ($R^2 = 0.67$) and the BDOC concentration model had the strongest relationship ($R^2 = 0.83$; Figure 3). Variance inflation factor was low for all parameters (<3) and the RESET, Breusch-Pagan, and Durbin-Watson tests were all nonsignificant, indicating acceptable colinearity, linearity, equal variance, and autocorrelation.
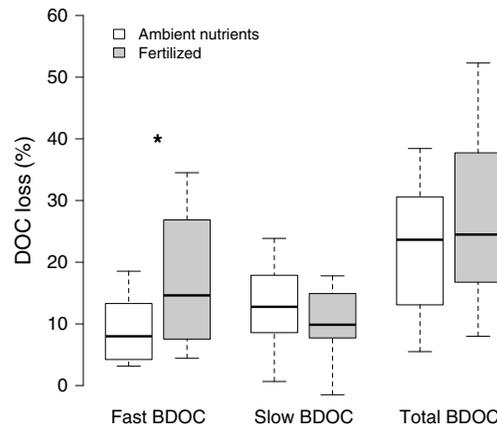

Figure 3. Fitted versus actual DOC loss (%) for a multiple linear regression model including PO_4^{3-}, $\delta^{18}O$, SUVA254, and NH_4^+ as independent variables. Models estimating fast, slow, and total BDOC are presented in Table 4. Shapes represent site type and shading represents activity level (defined in Figure 1).

Figure 4. DOC loss after 40 day incubation at room temperature. Fertilized vials were amended with 80 μM NH_4^+/NO_3^- and 10 μM PO_4^{3-}. Fast BDOC was defined as loss from $t_0 - t_{10}$, slow as loss from $t_{10} - t_{40}$, and total as loss from $t_0 - t_{40}$. Asterisk represents significant difference at $\alpha = 0.05$; $n = 7$ for each column. Symbology is defined in Figure 2.

We tested the effect of nutrient concentration on DOC processing by comparing amended and ambient nutrient incubations. The addition of inorganic N and P nearly doubled the amount of fast BDOC (SE = 3.48, $t(6) = 3.1$, $p = 0.02$), which averaged 9.2% for vials without added nutrients and 17.5% in amended incubations, but did not significantly affect slow BDOC (nonsignificant decrease of 2.7%, SE = 1.63, $t(6) = -1.64$, $p = 0.15$) or total BDOC (nonsignificant increase of 5.5%, SE = 3.01, $t(6) = 1.84$, $p = 0.12$; Figure 4). Furthermore, variation in the response to nutrient addition was positively correlated with DIN concentration ($R^2 = 0.79$, $F(1, 5) = 19.4$, $p = 0.007$), with sites higher in DIN showing a stronger response to nutrient addition (Δ fast BDOC (%) = 0.13 [DIN (μM)] + 1.5, Figure 5).

3.3. Feature and Vegetation Type

We compared BDOC by feature and vegetation type to test for differences due to how DOC is released from permafrost and original DOC source. Slumps were higher in BDOC than gullies ($F(1,29)$, $p = 0.026$) with adjusted means of 37.9% versus 25.0% total BDOC after controlling for differences in activity (Figure 6). BDOC differed with vegetation type independent of activity ($F(2,46)$, $p = 0.006$), with greater BDOC at sites located on moist nonacidic tundra compared to moist acidic tundra, with adjusted means of 36.6 and 21.2% total BDOC (Figure 7). $SUVA_{254}$ varied by vegetation ($F(2,44)$, $p = 0.0001$), with nonacidic sites lower than acidic sites with adjusted means of 4.3 and 2.2 L mg C^{-1} m^{-1}, but C:N ratio, DIN, and PO_4^{3-} did not significantly vary across vegetation types ($F(2, 28)$, $p = 0.28$, 0.43, and 0.44, respectively). For all parameters, shrubs were intermediate between acidic and nonacidic tundra and did not vary significantly from either type.

3.4. Seasonal Patterns of BDOC

While individual sites had high variability in BDOC between samplings through the season, there was no clear trend in BDOC seasonality for reference or impacted waters (Figure 8). The average of BDOC range (maximum–minimum values for an individual site over the season) varied by up to 50% with an overall average of 20.4% ($n = 12$, SE = 4.8). Impacted sites were more variable than reference water tracks with a mean BDOC range of 28.7% compared to the reference mean of 12.4% ($t(8.83) = -2.4$, $p = 0.04$). For the two gullies and water tracks where repeat measurements were taken at least monthly, BDOC was highest in the middle to late season (July and August). Lowest BDOC for all sites occurred early in the season on 15 June.
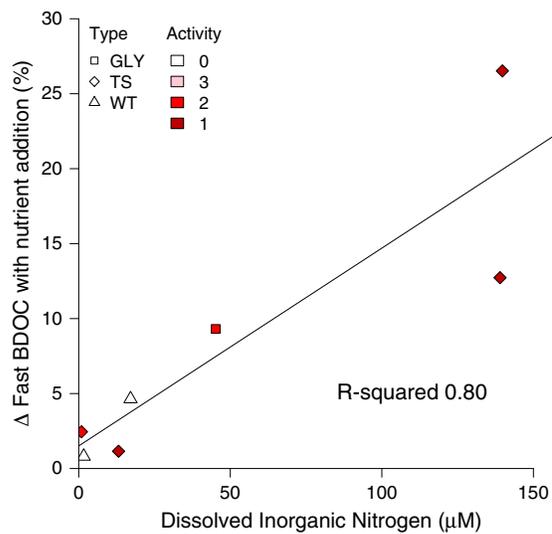
4. Discussion

4.1. Permafrost DOC Pools and Biodegradability

DOC from collapsing permafrost on the North Slope is some of the most biodegradable reported in natural systems. Across multiple vegetation types, landscape ages, and thermokarst morphologies, DOC from
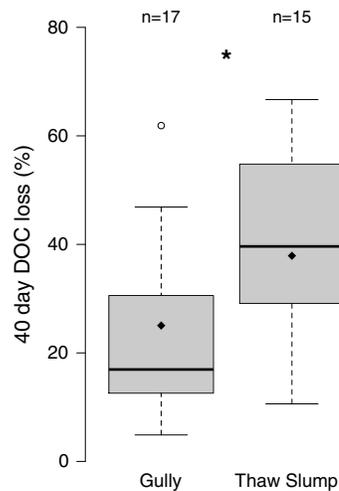

Figure 5. Response of fast BDOC (DOC loss from $t_0 - t_{10}$) to nutrient addition. Each point represents the fertilized DOC loss (%) minus the ambient nutrient DOC loss (%). Shapes represent site type and shading represents activity level (defined in Figure 1).

Figure 6. Comparison of BDOC between thaw slump and gully thermokarst features while controlling for activity level. Diamonds denote mean BDOC after adjusting for activity. Asterisk represents significant difference at $\alpha = 0.05$. Symbology is defined in Figure 2.
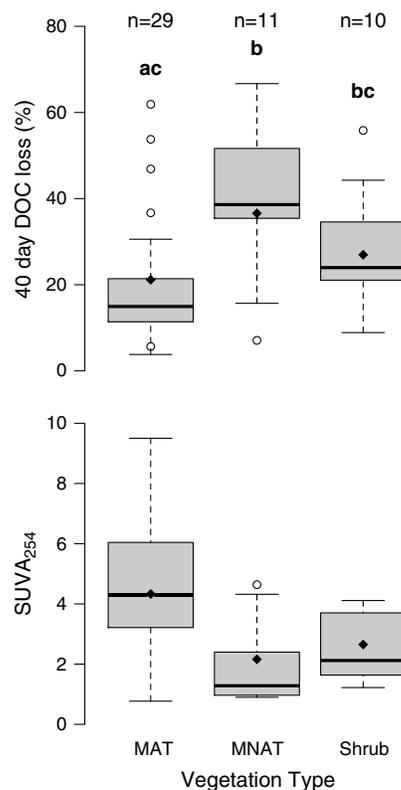

Figure 7. Comparison of BDOC and $SUVA_{254}$ between moist acidic tundra (MAT), moist nonacidic tundra (MNAT), and shrub tundra (Shrub), controlling for activity level. Diamonds denote mean BDOC after adjusting for activity. Different letters represent significant differences between activity levels, $\alpha = 0.05$.

permafrost is consistently more biodegradable than surface-derived DOC. High BDOC is accompanied by elevated DOC concentrations, resulting in extremely high rates of DOC mineralization from waters impacted by permafrost collapse. However, elevated BDOC only persists during active permafrost degradation, and BDOC returns to predisturbance levels once thermokarst features stabilize and start to revegetate. This finding informs the importance of thermokarst morphology in determining BDOC release from permafrost. Though gully and active layer detachment features are more common on the landscape and make up a larger portion of total thermokarst area [*Krieger*, 2012], they typically stabilize within a few years [*Godin and Fortier*, 2012; *Lewkowicz and Harris*, 2005]. Thaw slumps, however, can remain active for decades [*Lantuit et al.*, 2012; *Lantz and Kokelj*, 2008], mobilizing biodegradable permafrost DOC from meters below the surface.

4.2. DOC Composition

DOC aromaticity and C:N of DOM were negatively related to biodegradability, supporting our hypothesis that chemical composition of permafrost DOC contributes to its high biodegradability. The fact that fast and slow BDOC were poorly correlated and responded differently to nutrient addition is evidence that multiple pools of DOC with differing degrees of biodegradability are at play.

Arctic river DOC is typically most biodegradable during snowmelt [*Holmes et al.*, 2008; *Mann et al.*, 2012], when recently fixed vascular plant inputs dominate DOM sources [*Neff et al.*, 2006; *Spencer et al.*, 2008]. This DOM released during snowmelt has high $SUVA_{254}$ (~4.0), high C:N (>40), and has undergone little microbial processing due to rapid transport across frozen soil [*Holmes et al.*, 2012; *Mann et al.*, 2012; *Spencer et al.*, 2008]. In contrast, permafrost DOM has low $SUVA_{254}$ (1.9) and low C:N (21.7) in the range of soil or microbially derived DOM (10–25), suggesting considerable prior processing [*Amon and Meon*, 2004; *Amon et al.*, 2012; *Kawahigashi et al.*, 2004; *Neff et al.*, 2006]. Yet permafrost DOM is more biodegradable than DOM released during snowmelt. This inconsistency highlights the complexity of predicting BDOC, particularly when comparing fresh and degraded DOM. While the chemical composition of permafrost DOM is distinct from Arctic snowmelt DOM, it is similar to late-winter DOM in the Yukon basin, which has high BDOC (40%), low $SUVA_{254}$ (2.0), and low C:N (20.7) [*O'Donnell et al.*, 2012; *Wickland et al.*, 2012]. A possible explanation for this similarity is that some of the DOM in wintertime base flow is coming from permafrost via soil water, groundwater, or thermokarst inputs. The Yukon basin is underlain by discontinuous permafrost and has experienced substantial warming and changes in precipitation [*Chapin et al.*, 2010] with large areas
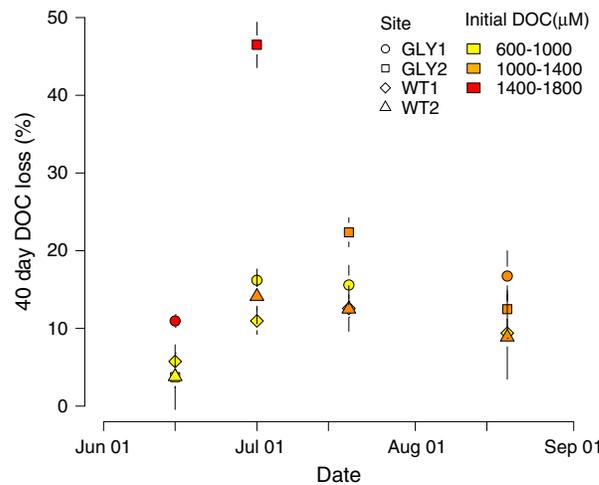
Figure 8. Seasonal patterns of DOC biodegradability for two gullies and two water tracks. Complete site information in Table 1. Shapes represent site type, and shading represents the initial DOC concentration. Error bars are ± SE of replicate incubation vials.

experiencing permafrost degradation [*Belshe et al.*, 2013; *Lu and Zhuang*, 2011; *Osterkamp*, 2005]. The only other published estimate of presnowmelt, riverine BDOC is from the Kolyma basin in Eastern Siberia, where BDOC was less than 5% [*Mann et al.*, 2012]. If permafrost DOM is the source of winter BDOC in the Yukon, this could explain the large difference between these catchments. The Kolyma is underlain by continuous permafrost and has experienced less severe summer and winter warming [*Chapin et al.*, 2005; *Serreze et al.*, 2000]; therefore, the contribution of permafrost DOM to winter BDOC should be relatively lower than in the Yukon.

4.3. Nutrients

Nutrient addition had mixed effects on BDOC, in line with previous findings [*Balczarczyk et al.*, 2009; *Holmes et al.*, 2008].

The fact that sites with high DIN showed a greater response to nutrient addition was contrary to our prediction that low-nutrient sites would respond most strongly and does not support the hypothesis that nutrient availability limits DOC processing. Because DIN is highly correlated with site activity, the relationship between DIN and response to nutrient addition may indicate that sites with more biodegradable, permafrost-derived DOC are more sensitive to nutrient addition. This interaction coincides, albeit on a much faster time scale, with observations of bulk soil C processing in tundra soil, where higher nutrient availability enhances labile C processing but suppresses recalcitrant C processing [*Lavoie et al.*, 2011].

Regression and correlation analysis revealed that inorganic nutrients, particularly PO_4^{3-} and NH_4^+, are associated with DOC biodegradability. These relationships were robust in predicting the biodegradability of both surface and permafrost-derived DOM (Figure 4), suggesting common controls on biodegradability, regardless of source. However, the fact that NH_4^+ was highly correlated with site activity may mean that its relationship with BDOC is partially or primarily correlative. PO_4^{3-} was relatively less correlated with activity and was generally a better predictor of BDOC, suggesting an influence on BDOC independent of activity. It is important to note that correlation and regression analysis was based on data from incubations with added nutrients. As such, relationships between initial nutrient concentration and BDOC are likely due to indirect correlations between nutrients and other factors such as vegetation type, flow path, DOM source, or micronutrients rather than direct effects of N or P on BDOC.

Mineral soil in the Arctic are enriched in inorganic N relative to organic soil [*Harms et al.*, 2013; *Keuper et al.*, 2012], and increased active layer depth could modify hydrologic flow paths, causing the simultaneous export of biodegradable permafrost DOC and DIN on a local or landscape scale [*Harms et al.*, 2013; *Jones et al.*, 2005; *Striegl et al.*, 2005; *Wickland et al.*, 2012]. Similarly, in the case of thermokarst, nutrient concentration is highly associated with feature activity, resulting in the features releasing the most permafrost DOC also releasing highest concentrations of inorganic nutrients. Another possibility explaining the correlation between BDOC and inorganic nutrients is that the nutrients associated with water rich in BDOC are at least partially derived from the DOM itself during mineralization.

4.4. Acidic and Nonacidic Tundra DOM Biodegradability

Sites draining moist nonacidic tundra sites had higher BDOC than those draining moist acidic tundra sites. This pattern may be due to more decomposable DOM inputs from nonacidic tundra or accelerated decomposition of DOM in acidic tundra soil before reaching the stream. While litter decay rates are similar between acidic and nonacidic tundra, decomposition can occur up to 84% more rapidly at acidic sites, potentially due to increased N availability and differences in microbial community [*Hobbie and Gough*, 2004;

Hobbie et al., 2005; *Nordin et al.*, 2004]. If DOM is processed faster in acidic tundra, a larger portion of BDOC would be consumed before reaching the stream or being incorporated into permafrost, leading to lower BDOC in moist acidic tundra ground ice and surface water. Alternatively, there is evidence that DOM biodegradability may be inversely correlated with biodegradability of the plant residue from which it leached. Litter from sedges decomposes fastest, followed by deciduous shrubs and mosses [*Hobbie*, 1996]. Leachate biodegradability follows the opposite pattern, with very high BDOC in moss-derived DOM, followed by deciduous shrubs and sedges [*Wickland et al.*, 2007]. If this pattern holds, DOM from nonacidic sites with lower litter and soil decay rates may have higher BDOC.

4.5. BDOC and Thermokarst Morphology

Differences in the biodegradability of DOC released from thaw slumps and gullies suggest that ground ice type influences BDOC (Figure 2). However, lower BDOC in gully outflow may be due to dilution of permafrost meltwater by surface water inputs, rather than differences in ground ice BDOC. Gullies often form in convergent topography with a larger upslope catchments than thaw slumps [*Krieger*, 2012]. Consequently, gully outflow has a lower proportion of permafrost versus surface-derived water and DOM. This explanation is supported by the fact that the gully with the highest BDOC (gully 7, Table 1) was the only one without surface water input.

4.6. Why Is Permafrost DOC So Biodegradable?

Different mechanisms potentially account for elevated BDOC in wedge and relic glacial ice formations, which are the most common ground ice types in our study area and are widespread throughout the Arctic [*French and Shur*, 2010; *Zhang et al.*, 1999]. Ice wedges form when spring runoff flows into surface cracks formed from thermal contraction during extreme cold in the previous winter [*Fortier and Allard*, 2004]. Because ice wedges are filled during the later stages of snowmelt [*Lauriol et al.*, 1995] the water that fills them is rich in the same litter and winter microbial activity-derived DOC that fuels patterns of high BDOC in Arctic surface waters during snowmelt. Over centuries and millennia this unprocessed spring leachate could build up in ice wedges, providing a labile BDOC source upon thaw. However, the low C:N and $SUVA_{254}$ of permafrost DOM suggests it is derived from microbial or soil sources as opposed to fresh plant matter. If snowmelt DOM is the major source of ice wedge DOM, considerable processing must take place during or after incorporation. As for the source of BDOC in buried glacial ice, modern glacial ice can contain highly biodegradable DOC derived from microbial production [*Hood et al.* 2009], which more closely matches the DOM characteristics we observed in thermokarst outflows. If such DOC was present when relic glacial ice was stranded and buried, microbially derived C could explain high BDOC in thaw slumps fueled by buried glacial ice. However, DOC concentrations in modern glacial ice are typically low, and ice ablation or another concentrating process would be necessary to produce the high concentrations of BDOC observed in thermokarst outflow.

If nutrient availability does not enhance BDOC, how can DOM from ground ice types such as ice wedges and transition ice be more biodegradable than the surface sources from which they derive? We hypothesize four potential mechanisms that could increase DOC biodegradability relative to modern DOC sources. First, permafrost mineral soil strongly sorbs hydrophobic C species, which tend to be recalcitrant [*Kawahigashi et al.*, 2006, 2004]. Upon permafrost thaw, the DOC available for export could have a higher biodegradability since the less bioavailable compounds have effectively been filtered by the mineral soil. Second, repeated freeze-thaw cycles can release highly biodegradable DOC from the microbial community [*Schimel and Clein*, 1996]. This release is typically taken up rapidly or respired by microorganisms that survived the cycle [*Schimel and Clein*, 1996]. However, if these pulses of bioavailable DOC were released near a freezing front at the permafrost table or near an ice wedge crack they could be incorporated into ground ice. Third, microbial metabolism has been shown to continue well below the freezing point [*Wilhelm et al.*, 2012], and it is not known what portion of microbial biomass and metabolites is incorporated into permafrost as DOC rather than respired. Although microbial metabolism rates are low at temperatures typical of continuous permafrost—processing $1–2\,\mu g\,g^{-1}\,C\,d^{-1}$ [*Mikan et al.*, 2002; *Osterkamp*, 2005]—subzero metabolism could process a substantial portion of available soil organic matter over several millennia. Incomplete breakdown of frozen soil organic matter, either during freeze-thaw cycles or subzero metabolism, could lead to the accumulation of simple carbon compounds such as acetate, which could explain the low C:N and $SUVA_{254}$ of permafrost-derived DOM. Finally, some vegetation paleocommunities may have produced relatively biodegradable DOM compared to modern communities. This seems a likely explanation for the extremely high BDOC in Pleistocene-aged

loess deposits where C derives primarily from grasses [*Zimov et al.*, 2006]. However, for other permafrost types on the North Slope, pollen records reveal spatially heterogeneous community shifts, rather than a landscape-scale pattern of more biodegradable DOM sources [*Anderson et al.*, 1994; *Fritz et al.*, 2012; *Oswald et al.*, 2003].

An additional factor not considered here, which may further enhance DOC mineralization after release from permafrost, is high photodegradability of permafrost DOM when exposed to sunlight after reaching the surface [*Cory et al.*, 2013]. Several features included in our study (ALD 1, gullies 1 and 2, and thaw slumps 2–4 and 8) showed more than a 40% increase in microbial conversion of DOC to CO_2 when exposed to sunlight [*Cory et al.*, 2013]. Actual rates of permafrost DOC mineralization may be higher than measured in our dark incubations in field conditions when exposed to sunlight.

5. Conclusions

As the Arctic warms, DOC from thawing permafrost will play an increasingly important role governing freshwater and estuarine C and nutrient dynamics through the season. The overall ecological importance of thermokarst BDOC depends on the number of features, their location on the landscape, and the length of their active period. Approximately a third of permafrost has ice content in excess of 10% [*Zhang et al.*, 1999] and is susceptible to thermokarst upon thaw [*Jorgenson et al.*, 2006]. With up to 80% of near surface permafrost projected to degrade by 2100 if human greenhouse gas emissions are not reduced [*Slater and Lawrence*, 2013], thermokarst could impact up to $5.5 \times 10^6 \, km^2$ by the end of the century.

Since thermal disturbance from flowing or standing water often triggers gully and thaw slump formation, thermokarst may be the dominant short-term mechanism delivering sediment, nutrients, and biodegradable organic matter to aquatic systems as the Arctic warms. This could have significant local, landscape, and global consequences [*Bowden et al.*, 2008; *Thienpont et al.*, 2013]. Thermokarst outflow is most active when temperature is high in the middle to late summer, precisely when Arctic surface water BDOC is lowest [*Holmes et al.*, 2008; *Mann et al.*, 2012; *Wickland et al.*, 2012]. Chronic loading of BDOC from widespread thermokarst could cause a substantial shift in late-season DOC dynamics in Arctic streams, lakes, and estuaries. Permafrost BDOC release could also be important for the global C cycle, enhancing the permafrost C feedback due to direct CO_2 release from the decomposition of permafrost DOC and enhanced heterotrophic processing of nonpermafrost DOC due to the priming effect [*Bianchi*, 2011; *Guenet et al.*, 2010].

High lability of permafrost DOC should be considered when estimating changes in DOC delivery to aquatic ecosystems. Due to substantial DOC losses on time scales less than residence time of many Arctic waters, monitoring of river mouth or estuarine DOC could miss a large portion of DOC released from degrading permafrost which was processed in transit.

References

Amon, R. M. W., and B. Meon (2004), The biogeochemistry of dissolved organic matter and nutrients in two large Arctic estuaries and potential implications for our understanding of the Arctic Ocean system, *Mar. Chem.*, 92(1-4), 311–330.

Amon, R. M. W., et al. (2012), Dissolved organic matter sources in large Arctic rivers, *Geochim. Cosmochim. Acta*, 94, 217–237.

Anderson, P. M., P. J. Bartlein, and L. B. Brubaker (1994), Late Quaternary history of tundra vegetation in northwestern Alaska, *Quat. Res.*, 41(3), 306–315.

Aufdenkampe, A. K., E. Mayorga, P. A. Raymond, J. M. Melack, S. C. Doney, S. R. Alin, R. E. Aalto, and K. Yoo (2011), Riverine coupling of biogeochemical cycles between land, oceans, and atmosphere, *Front. Ecol. Environ.*, 9(1), 53–60.

Balcarczyk, K. L., J. B. Jones, R. Jaffe, and N. Maie (2009), Stream dissolved organic matter bioavailability and composition in watersheds underlain with discontinuous permafrost, *Biogeochemistry*, 94(3), 255–270.

Belshe, E. F., E. A. G. Schuur, and G. Grosse (2013), Quantification of upland thermokarst features with high resolution remote sensing, *Environ. Res. Lett.*, 8(3), doi:10.1088/1748-9326/8/3/035016.

Bianchi, T. S. (2011), The role of terrestrially derived organic carbon in the coastal ocean: A changing paradigm and the priming effect, *Proc. Natl. Acad. Sci. U.S.A.*, 108(49), 19,473–19,481.

Bowden, W. B., M. N. Gooseff, A. Balser, A. Green, B. J. Peterson, and J. Bradford (2008), Sediment and nutrient delivery from thermokarst features in the foothills of the North Slope, Alaska: Potential impacts on headwater stream ecosystems, *J. Geophys. Res.*, 113, G02026, doi:10.1029/2007JG000470.

Chapin, F. S., et al. (2005), Role of land-surface changes in Arctic summer warming, *Science*, 310(5748), 657–660.

Chapin, F. S., et al. (2010), Resilience of Alaska's boreal forest to climatic change, *Can. J. For. Res. -Revue Canadienne De Recherche Forestiere*, 40(7), 1360–1370.

Cory, R. M., B. C. Crump, J. A. Dobkowski, and G. W. Kling (2013), Surface exposure to sunlight stimulates CO_2 release from permafrost soil carbon in the Arctic, *Proc. Natl. Acad. Sci. U.S.A.*, 110(9), 3429–3434.

Dery, S. J., M. Stieglitz, A. K. Rennermalm, and E. F. Wood (2005), The water budget of the Kuparuk River basin, Alaska, *J. Hydrometeorol.*, 6(5), 633–655.

Fortier, D., and M. Allard (2004), Late Holocene syngenetic ice-wedge polygons development, Bylot Island, Canadian Arctic Archipelago, *Can. J. Earth Sci.*, *41*(8), 997–1012.

Frampton, A., S. Painter, S. W. Lyon, and G. Destouni (2011), Non-isothermal, three-phase simulations of near-surface flows in a model permafrost system under seasonal variability and climate change, *J. Hydrol.*, *403*(3–4), 352–359.

French, H., and Y. Shur (2010), The principles of cryostratigraphy, *Earth Sci. Rev.*, *101*(3), 190–206.

Frey, K. E., and J. W. McClelland (2009), Impacts of permafrost degradation on Arctic river biogeochemistry, *Hydrol Process*, *23*(1), 169–182.

Fritz, M., U. Herzschuh, S. Wetterich, H. Lantuit, G. P. De Pascale, W. H. Pollard, and L. Schirrmeister (2012), Late glacial and Holocene sedimentation, vegetation, and climate history from easternmost Beringia (northern Yukon Territory, Canada), *Quat. Res*, *78*(3), 549–560.

Godin, E., and D. Fortier (2012), Geomorphology of a thermo-erosion gully, Bylot Island, Nunavut, Canada, *Can. J. Earth Sci.*, *49*(8), 979–986.

Guenet, B., M. Danger, L. Abbadie, and G. Lacroix (2010), Priming effect: Bridging the gap between terrestrial and aquatic ecology, *Ecology*, *91*(10), 2850–2861.

Hamilton, T. (2003), *Surficial Geology of the Dalton Highway (Itkillik-Sagavanirktok rivers) Area, Southern Arctic Foothills*, Alaska Div. of Geol. and Geophys. Surv., Fairbanks.

Harms, T., B. Abbott, and J. Jones (2013), Thermo-erosion gullies increase nitrogen available for hydrologic export, *Biogeochemistry*, *117*, 299–311.

Hobbie, S. E. (1996), Temperature and plant species control over litter decomposition in Alaskan tundra, *Ecol. Monogr.*, *66*(4), 503–522.

Hobbie, S. E., and L. Gough (2004), Litter decomposition in moist acidic and non-acidic tundra with different glacial histories, *Oecologia*, *140*(1), 113–124.

Hobbie, S. E., L. Gough, and G. R. Shaver (2005), Species compositional differences on different-aged glacial landscapes drive contrasting responses of tundra to nutrient addition, *J. Ecol.*, *93*(4), 770–782.

Hood, E., et al. (2009), Glaciers as a source of ancient and labile organic matter to the marine environment, *Nature*, *462*, 1044–1047, doi:10.1038/Nature08580.

Holmes, R. M., J. W. McClelland, P. A. Raymond, B. B. Frazer, B. J. Peterson, and M. Stieglitz (2008), Lability of DOC transported by Alaskan rivers to the arctic ocean, *Geophys. Res. Lett.*, *35*, L03402, doi:10.1029/2007GL032837.

Holmes, R. M., et al. (2012), Seasonal and annual fluxes of nutrients and organic matter from large rivers to the Arctic Ocean and surrounding seas, *Estuaries Coasts*, *35*(2), 369–382.

Jones, J. B., K. C. Petrone, J. C. Finlay, L. D. Hinzman, and W. R. Bolton (2005), Nitrogen loss from watersheds of interior Alaska underlain with discontinuous permafrost, *Geophys. Res. Lett.*, *32*, L02401, doi:10.1029/2004GL021734.

Jorgenson, M. T., and T. E. Osterkamp (2005), Response of boreal ecosystems to varying modes of permafrost degradation, *Can. J. For. Res. -Revue Canadienne De Recherche Forestiere*, *35*(9), 2100–2111.

Jorgenson, M. T., Y. L. Shur, and E. R. Pullman (2006), Abrupt increase in permafrost degradation in Arctic Alaska, *Geophys. Res. Lett.*, *33*, L02503, doi:10.1029/2005GL024960.

Jorgenson, M. T., Y. L. Shur, and T. E. Osterkamp (2008), Thermokarst in Alaska, in *Ninth International Conference on Permafrost*, pp. 117–124, Univ. of Alaska, Fairbanks.

Jorgenson, M. T., J. E. Roth, P. F. Miller, M. J. Macander, M. S. Duffy, A. F. Wells, G. V. Frost, and E. R. Pullman (2009), An ecological land survey and landcover map of the Arctic network, *Natural Resource Tech. Rep. NPS/ARCN/NRTR—2009/270*, Natl. Park Serv., Fort Collins, Colo.

Kalbitz, K., J. Schmerwitz, D. Schwesig, and E. Matzner (2003), Biodegradation of soil-derived dissolved organic matter as related to its properties, *Geoderma*, *113*(3-4), 273–291.

Kawahigashi, M., K. Kaiser, K. Kalbitz, A. Rodionov, and G. Guggenberger (2004), Dissolved organic matter in small streams along a gradient from discontinuous to continuous permafrost, *Global Change Biol.*, *10*(9), 1576–1586.

Kawahigashi, M., K. Kaiser, A. Rodionov, and G. Guggenberger (2006), Sorption of dissolved organic matter by mineral soils of the Siberian forest tundra, *Global Change Biol.*, *12*(10), 1868–1877.

Keuper, F., P. M. van Bodegom, E. Dorrepaal, J. T. Weedon, J. van Hal, R. S. P. van Logtestijn, and R. Aerts (2012), A frozen feast: thawing permafrost increases plant-available nitrogen in subarctic peatlands, *Global Change Biol.*, *18*(6), 1998–2007.

Kokelj, S. V., and M. T. Jorgenson (2013), Advances in thermokarst research, *Permafrost Periglac Processes*, *24*(2), 108–119, doi:10.1002/ppp.1779.

Krieger, K. C. (2012), The topographic form and evolution of thermal erosion features: A first analysis using airborne and ground-based LiDAR in Arctic Alaska, MS thesis, Dep. of Geosci., Idaho State Univ., Pocatello.

Lantuit, H., W. H. Pollard, N. Couture, M. Fritz, L. Schirrmeister, H. Meyer, and H. W. Hubberten (2012), Modern and Late Holocene retrogressive thaw slump activity on the Yukon Coastal Plain and Herschel Island, Yukon Territory, Canada, *Permafrost Periglac Processes*, *23*(1), 39–51.

Lantz, T. C., and S. V. Kokelj (2008), Increasing rates of retrogressive thaw slump activity in the Mackenzie Delta Region, NWT, Canada, *Geophys. Res. Lett.*, *35*, L06502, doi:10.1029/2007GL032433.

Lauriol, B., C. Duchesne, and I. D. Clark (1995), Systématique du Remplissage en Eau des Fentes de Gel: Les Résultats d'une Étude Oxygène-18 et Deutérium, *Permafrost Periglac Processes*, *6*(1), 47–55.

Lavoie, M., M. C. Mack, and E. A. G. Schuur (2011), Effects of elevated nitrogen and temperature on carbon and nitrogen dynamics in Alaskan arctic and boreal soils, *J. Geophys. Res.*, *116*, G03013, doi:10.1029/2010JG001629.

Lewkowicz, A. G., and C. Harris (2005), Frequency and magnitude of active-layer detachment failures in discontinuous and continuous permafrost, northern Canada, *Permafrost Periglac Processes*, *16*(1), 115–130.

Lu, X. L., and Q. L. Zhuang (2011), Areal changes of land ecosystems in the Alaskan Yukon River Basin from 1984 to 2008, *Environ. Res. Lett.*, *6*(3), doi:10.1088/1748-9326/6/3/034012.

Mann, P. J., A. Davydova, N. Zimov, R. G. M. Spencer, S. Davydov, E. Bulygina, S. Zimov, and R. M. Holmes (2012), Controls on the composition and lability of dissolved organic matter in Siberia's Kolyma River basin, *J. Geophys. Res.*, *117*, G01028, doi:10.1029/2011JG001798.

McDowell, W. H., A. Zsolnay, J. A. Aitkenhead-Peterson, E. G. Gregorich, D. L. Jones, D. Jodemann, K. Kalbitz, B. Marschner, and D. Schwesig (2006), A comparison of methods to determine the biodegradable dissolved organic carbon from different terrestrial sources, *Soil Biol. Biochem.*, *38*(7), 1933–1942.

McGuire, A. D., L. G. Anderson, T. R. Christensen, S. Dallimore, L. Guo, D. J. Hayes, M. Heimann, T. D. Lorenson, R. W. Macdonald, and N. Roulet (2009), Sensitivity of the carbon cycle in the Arctic to climate change, *Ecol. Monogr.*, *79*(4), 523–555.

McNamara, J. P., D. L. Kane, and L. D. Hinzman (1998), An analysis of streamflow hydrology in the Kuparuk River basin, Arctic Alaska: A nested watershed approach, *J. Hydrol.*, *206*(1-2), 39–57.

Michaelson, G. J., C. L. Ping, G. W. Kling, and J. E. Hobbie (1998), The character and bioactivity of dissolved organic matter at thaw and in the spring runoff waters of the Arctic tundra north slope, Alaska, *J. Geophys. Res.*, *103*(D22), 28,939–28,946, doi:10.1029/98JD02650.

Mikan, C. J., J. P. Schimel, and A. P. Doyle (2002), Temperature controls of microbial respiration in Arctic tundra soils above and below freezing, *Soil Biol. Biochem.*, *34*(11), 1785–1795.

Neff, J. C., J. C. Finlay, S. A. Zimov, S. P. Davydov, J. J. Carrasco, E. A. G. Schuur, and A. I. Davydova (2006), Seasonal changes in the age and structure of dissolved organic carbon in Siberian Rivers and Streams, *Geophys. Res. Lett.*, *33*, L23401, doi:10.1029/2006GL028222.

Nordin, A., I. K. Schmidt, and G. R. Shaver (2004), Nitrogen uptake by Arctic soil microbes and plants in relation to soil nitrogen supply, *Ecology*, *85*(4), 955–962.

O'Donnell, J. A., G. R. Aiken, M. A. Walvoord, and K. D. Butler (2012), Dissolved organic matter composition of winter flow in the Yukon River basin: Implications of permafrost thaw and increased groundwater discharge, *Global Biogeochem. Cycles*, *26*, GB0E06, doi:10.1029/2012GB004341.

Osterkamp, T. E. (2005), The recent warming of permafrost in Alaska, *Global Planet. Change*, *49*(3-4), 187–202.

Osterkamp, T. E., M. T. Jorgenson, E. A. G. Schuur, Y. L. Shur, M. Z. Kanevskiy, J. G. Vogel, and V. E. Tumskoy (2009), Physical and ecological changes associated with warming permafrost and thermokarst in interior Alaska, *Permafrost Periglac Processes*, *20*(3), 235–256.

Oswald, W. W., L. B. Brubaker, F. S. Hu, and G. W. Kling (2003), Holocene pollen records from the central Arctic Foothills, northern Alaska: Testing the role of substrate in the response of tundra to climate change, *J. Ecol.*, *91*(6), 1034–1048.

Schimel, J. P., and J. S. Clein (1996), Microbial response to freeze-thaw cycles in tundra and taiga soils, *Soil Biol. Biochem.*, *28*(8), 1061–1066.

Serreze, M. C., J. E. Walsh, F. S. Chapin, T. Osterkamp, M. Dyurgerov, V. Romanovsky, W. C. Oechel, J. Morison, T. Zhang, and R. G. Barry (2000), Observational evidence of recent change in the northern high-latitude environment, *Clim. Change*, *46*(1–2), 159–207.

Slater, A. G., and D. M. Lawrence (2013), Diagnosing present and future permafrost from climate models, *J. Clim.*, *26*(15), 5608–5623, doi:10.1175/jcli-d-12-00341.1.

Spencer, R. G. M., G. R. Aiken, K. P. Wickland, R. G. Striegl, and P. J. Hernes (2008), Seasonal and spatial variability in dissolved organic matter quantity and composition from the Yukon River basin, Alaska, *Global Biogeochem. Cycles*, *22*, GB4002, doi:10.1029/2008GB003231.

Striegl, R. G., G. R. Aiken, M. M. Dornblaser, P. A. Raymond, and K. P. Wickland (2005), A decrease in discharge-normalized DOC export by the Yukon River during summer through autumn, *Geophys. Res. Lett.*, *32*, L21413, doi:10.1029/2005GL024413.

Tank, S. E., K. E. Frey, R. G. Striegl, P. A. Raymond, R. M. Holmes, J. W. McClelland, and B. J. Peterson (2012), Landscape-level controls on dissolved carbon flux from diverse catchments of the circumboreal, *Global Biogeochem. Cycles*, *26*, GB0E02, doi:10.1029/2012GB004299.

Tarnocai, C., J. G. Canadell, E. A. G. Schuur, P. Kuhry, G. Mazhitova, and S. Zimov (2009), Soil organic carbon pools in the northern circumpolar permafrost region, *Global Biogeochem. Cycles*, *23*, GB2023, doi:10.1029/2008GB003327.

Thienpont, J. R., K. M. Ruehland, M. F. J. Pisaric, S. V. Kokelj, L. E. Kimpe, J. M. Blais, and J. P. Smol (2013), Biological responses to permafrost thaw slumping in Canadian Arctic lakes, *Freshwater Biol.*, *58*(2), 337–353.

Toolik Environmental Data Center Team (2011), Meterological monitoring program at Toolik, Alaska, Toolik Field Station, Inst. of Arctic Biol., Univ. of Alaska Fairbanks, Fairbanks.

Vonk, J. E., et al. (2013), High biolability of ancient permafrost carbon upon thaw, *Geophys. Res. Lett.*, *40*, 2689–2693, doi:10.1002/grl.50348.

Walker, D. A. et al. (2005), The Circumpolar Arctic vegetation map, *J. Vegetation Sci.*, *16*, 267–282, doi:10.1111/j.1654-1103.2005.tb02365.x.

Weishaar, J. L., G. R. Aiken, B. A. Bergamaschi, M. S. Fram, R. Fujii, and K. Mopper (2003), Evaluation of specific ultraviolet absorbance as an indicator of the chemical composition and reactivity of dissolved organic carbon, *Environ. Sci. Technol.*, *37*(20), 4702–4708.

Wickland, K. P., J. C. Neff, and G. R. Aiken (2007), Dissolved organic carbon in Alaskan boreal forest: Sources, chemical characteristics, and biodegradability, *Ecosystems*, *10*(8), 1323–1340.

Wickland, K. P., G. R. Aiken, K. Butler, M. M. Dornblaser, R. G. M. Spencer, and R. G. Striegl (2012), Biodegradability of dissolved organic carbon in the Yukon River and its tributaries: Seasonality and importance of inorganic nitrogen, *Global Biogeochem. Cycles*, *26*, GB0E03, doi:10.1029/2012GB004342.

Wilhelm, R. C., K. J. Radtke, N. C. S. Mykytczuk, C. W. Greer, and L. G. Whyte (2012), Life at the wedge: The activity and diversity of Arctic ice wedge microbial communities, *Astrobiology*, *12*(4), 347–360.

Woods, G. C., M. J. Simpson, B. G. Pautler, S. F. Lamoureux, M. J. Lafreniere, and A. J. Simpson (2011), Evidence for the enhanced lability of dissolved organic matter following permafrost slope disturbance in the Canadian High Arctic, *Geochim. Cosmochim. Acta*, *75*(22), 7226–7241.

Western Regional Climate Center (2011), Western Regional Climate Center. [Available at http://www.wrcc.dri.edu/.]

Zhang, T., R. G. Barry, K. Knowles, J. A. Heginbottom, and J. Brown (1999), Statistics and characteristics of permafrost and ground ice distribution in the Northern Hemisphere, *Polar Geogr.*, *23*(2), 147–169.

Zhang, Z., D. L. Kane, and L. D. Hinzman (2000), Development and application of a spatially-distributed Arctic hydrological and thermal process model (ARHYTHM), *Hydrol. Process.*, *14*(6), 1017.

Zimov, S. A., S. P. Davydov, G. M. Zimova, A. I. Davydova, E. A. G. Schuur, K. Dutta, and F. S. Chapin (2006), Permafrost carbon: Stock and decomposability of a globally significant carbon pool, *Geophys. Res. Lett.*, *33*, L20502, doi:10.1029/2006GL027484.